Article

Microstructure and Mechanical Properties of Al-5Mg-0.8Mn Alloys with Various Contents of Fe and Si Cast under Near-Rapid Cooling

Yulin Liu * [ID], Yimeng Sun, Li Zhang, Yuhua Zhao, Jijie Wang and Chunzhong Liu

Liaoning Provincial Key Laboratory of Light Alloys and Processing Technology, School of Materials Science and Engineering, Shenyang Aerospace University, 37 Daoyi Avenue S., Shenyang 110136, China; ymengsun@sina.com (Y.S.); zhangli@sau.edu.cn (L.Z.); zhaoyuhua2010@sau.edu.cn (Y.Z.); wangjijie@sau.edu.cn (J.W.); czliu@sau.edu.cn (C.L.)
* Correspondence: ylliu@sau.edu.cn; Tel.: +86-133-5243-6226

Abstract: Al-5Mg-0.8Mn alloys (AA5083) with various iron and silicon contents were cast under near-rapid cooling and rolled into sheets. The aim was to study the feasibility of minimizing the deteriorating level of the harmful Fe-rich phases on the mechanical properties through refining the intermetallics by significantly increasing the casting rate. The results showed that the size and density of the intermetallic particles that remained in the hot bands and the cold rolled sheets increased as the contents of iron and silicon in the alloys were increased. However, the increment of the particle sizes was limited due to the significant refinement of the intermetallics formed during casting under near-rapid cooling. The mechanical properties of the alloys reduced as the contents of iron and silicon in the alloys increased. However, the decrement of tensile strengths and ductility was quite small. Therefore, higher contents of iron and silicon could be used in the Al-5Mg-0.8Mn alloy (AA5083 alloy) when the material is cast under near-rapid cooling, such as in the continuous strip casting process.

Keywords: aluminum alloy; AA5083 alloy; intermetallic; microstructure; mechanical properties; near-rapid solidification

1. Introduction

The AA5083 alloy has been widely used in the construction, packaging, automotive and marine industries due to its many great advantages, such as good ductility, formability, weldability, toughness and corrosion resistance. It is an Al-Mg based aluminum alloy with an intermediate level of Mg content (4–5 wt %) and a relatively high content of Mn (0.4–1.0 wt %) [1]. Fe and Si are the main impurities. In aluminum alloys, Fe is usually combined with other elements to form Fe-rich intermetallics during solidification. In the AA5083 type Al-Mg-Mn alloy, Fe united with Mn to form coarse intermetallic $Al_6(Fe,Mn)$ [2]. The Fe-rich intermetallics displayed platelet-like morphologies. This type of Fe-rich intermetallics have often been regarded as most detrimental to the tensile properties of Al alloy due to its brittle nature and stress concentration created by the needle-like characteristic [3–5]. Therefore, in order to prevent the formation of coarse Fe-rich intermetallic phases, Fe has usually been limited to a very low level, such as 0.15 wt %. The composition specifications of AA5083 alloy for Fe and Si are 0.4 wt % [1]. The actual controlling limit in production practice is significantly lower. The low limits of the Fe and Si contents limits the use of recycled aluminum since the recycled materials usually contain high levels of Fe and Si, normally higher than 0.5 wt % Fe and 0.5 wt % Si. Undoubtedly, the low limits of the Fe and Si contents in the AA5083 alloy would greatly inflate the manufacturing cost of the materials and limit their broad application.

In order to minimize the detrimental effect of Fe, Mn is usually employed in the Al-Mg based alloy to modify the Fe-rich intermetallics from platelet-like shape into Chinese script shape, which is considered less detrimental to the mechanical properties of the alloy [6,7]. However, the excess Mn in the alloy would combine with Fe to form Mn- and Fe-rich intermetallic compounds which also deteriorated the mechanical properties. Finding a method to refine the Fe- and Mn-rich intermetallic is important and necessary for the improvement of the alloy.

Extensive research to improve the AA5083 alloy had been conducted with emphasis on the microstructures and mechanical properties [8–11], superplasticity [12–15], ultrafine grain [16–20] and adding element [21–24], etc. Recently, research was carried out on the formation of the Fe- and Mn-rich intermetallics in the AA5083 type Al-Mg-Mn alloy [2]. It was found that the Fe- and Mn-rich intermetallic could be significantly refined when the alloy was cast under near-rapid cooling. In the high Fe and Si contents alloys, the Fe- and Mn-rich intermetallic had been transformed into $Al_{15}(Fe,Mn)_3Si$, which was a quaternary phase in the form of fine fish bone or Chinese script. The effect of the microstructure changes on the mechanical properties of the alloy had not yet been evaluated. If the harmful effect of the intermetallics on the mechanical properties could be minimized by refining their size and modifying their morphologies, then, higher contents of Fe and Si could be tolerated in the alloy and, thus, a higher percentage of recycled aluminum alloy with higher contents of Fe and Si could be employed without significantly deteriorating the mechanical properties of the alloy. Thus, the production cost could be reduced. Therefore, it is of significant theoretical interest and commercial value to investigate the effect of Fe and Si on the mechanical properties of the alloy cast under near-rapid cooling.

AA5083 Al alloy sheet materials are often manufactured using the continuous strip casting (CC) technology. In the CC technology, the molten alloy is continuously fed into a moving mold to produce a cast slab. The moving mold is structured by two parallel steel belts which are continuously moving and cooled by injecting cold water from the two sides. The slab is cast under the cooling rate of 10^0–10^2 °C·s^{-1}, which is in the range of near-rapid cooling.

So far, a lot of research has been conducted to investigate the continuously strip cast materials [25–29]. However, little research had been done to study the refinement of the intermetallic by near-rapid cooling and their influence on the mechanical properties. To better understand the effect of the contents of Fe and Si on the mechanical properties of the alloy cast under near-rapid cooling, an Al-5Mg-0.8Mn alloy, which is a simplified composition of the AA5083, was designed with various Fe and Si contents. The study was focused on the influences of the contents of Fe and Si (both individual and combined) on the microstructure and mechanical properties of the alloy.

2. Experimental Procedures

In order to reach a high cooling rate similar to the cooling conditions in the CC technology, a casting apparatus with double-side water cooling was designed and made in lab. Figure 1 shows the schematic sketch of the apparatus. The casting mold was sized at 150 mm × 150 mm × 15 mm and continuously cooled by injecting cold water from two sides. The cooling rates of the cast slabs were determined by recording the evolution of temperature during cooling. The average cooling rates before the beginning of solidification were about 20 °C·s^{-1} which was computed from the approximate straight line portion of the cooling curve by using the formula dT/dt.
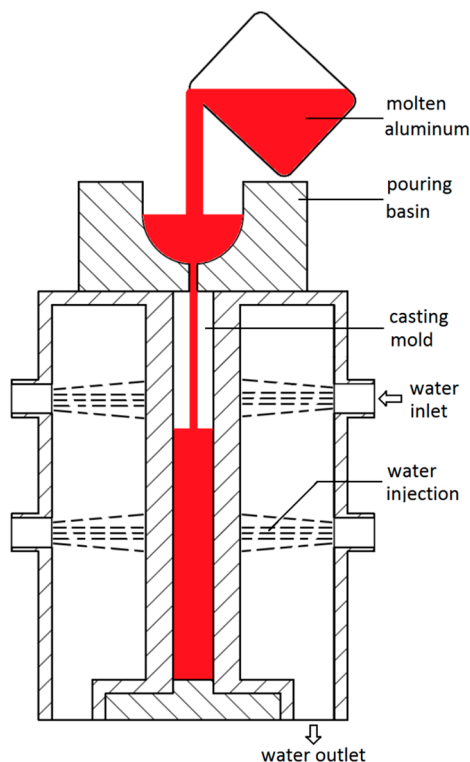
Figure 1. Schematic sketch of the double-side water cooled casting apparatus.

Four Al-5Mg-0.8Mn alloys with different Fe and Si levels were cast. The contents of Fe and Si in the alloys varied from less than 0.1 to 0.5 wt %. Pure Al ingots (Fe < 0.10 wt % and Si < 0.04 wt %), Mg ingots (99.9 wt %), Al-30Si and Al-10Fe mater alloys were employed to create the experimental alloy samples. For each alloy sample, two kilograms of raw materials were melted in an electric resistance furnace (General Furnace, Shenyang, China). The crucibles used were made of graphite-clay. The molten Al alloy was refined by adding 0.1% grain refiner (Al-5Ti-B), degassed by injecting Ar into the pool, then cast at around 725 °C by using the apparatus shown in Figure 1. The chemical compositions of the cast alloys were analyzed by emission spectroscopy and listed in Table 1.

Table 1. Chemical composition of the alloys, wt %.

| Alloy	Mg	Mn	Fe	Si	Cr	Ti	Zn	Cu	Al
Alloy 1	5.19	0.80	0.092	0.035	0.006	0.015	0.011	0.002	Bal.
Alloy 2	5.02	0.88	0.286	0.033	0.006	0.022	0.011	0.001	Bal.
Alloy 3	4.87	0.74	0.485	0.241	0.006	0.023	0.011	0.001	Bal.
Alloy 4	5.08	0.81	0.504	0.489	0.006	0.026	0.011	0.002	Bal.

The cast slabs were heated at 420 °C and hot rolled to 3.5 mm in thickness. The total reduction rate was 75%. Then, the hot bands were annealed for 2 h at 420 °C and then cold rolled to 1.4 mm in thickness. The reduction rate was 60%. Then, the cold rolled sheets were stabilizing treated at 150 °C for 2 h. Tensile tests were carried out for all the annealed hot bands as well as the stabilization treated cold rolled sheets. The tensile specimens with gauge width of 12 mm and length of 50 mm were cut from the sheets. The tensile direction was parallel to the rolling direction. Tensile tests were performed at a tensile speed of 2 mm/min.

The metallographic structures of the sheets were examined. The samples for metallographic observation were grinded with sandpapers and electropolished in a 60 mL $HClO_4$ + 140 mL H_2O + 800 mL C_2H_5OH solution at 27 V D.C. for 15 s. The grain structures were observed under

polarized light microscopy. The samples for polarizing light observation were anodized in Barker's reagent (50 mL HBF_4 + 950 mL H_2O at 18 V D.C. for 60 s. An Olympus GX71 optical microscope (Olympus Corporation, Shinjuku, Japan) with polarized light was used for the metallographic observations. A Zeiss scanning electron microscopy (SEM) (Zeiss Group, Oberkochen, Germany) and a Hitachi SEM (Hitachi, Tokyo, Japan) with energy dispersive X-ray (EDX) analyzer were utilized to observe the fracture surface of the tensile specimens and identify intermetallic compounds.

3. Results

The contents of Fe and Si and the cooling rate had significant influence on the as-cast microstructures of the alloys. In the low Fe and Si containing alloy, the intermetallics that precipitated during casting were small in both amount and size. They gradually increased with the increase of the contents of Fe and Si. In the high Fe and Si containing alloy (Alloy 4), the intermetallics formed during slow cooling were very massive, as shown in Figure 2. They became very fine when the alloy was cast under the condition of near-rapid cooling. To compare, Figure 2 also shows the fine intermetallics in Alloy 4. It can be seen that the intermetallics are extremely refined by the fast cooling. The detailed analyses on the intermetallics of all the alloys are reported in reference [2].
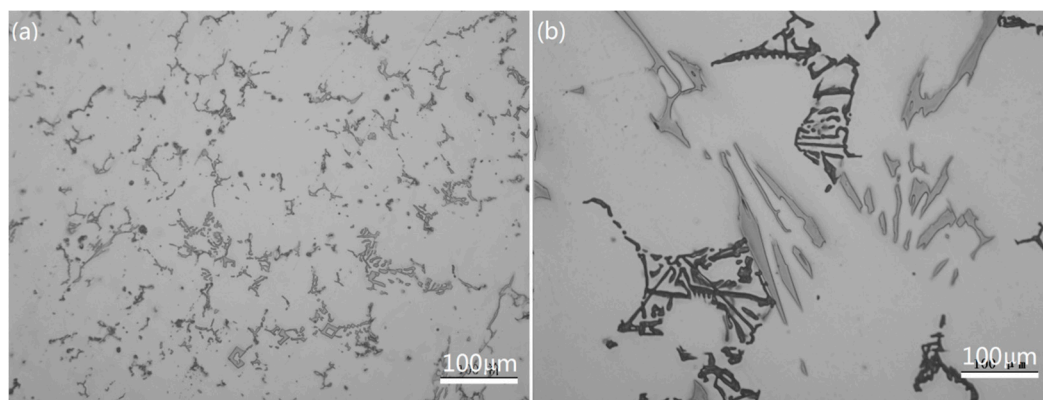

Figure 2. The as-cast microstructures of Alloy 4 cast under (**a**) near-rapid cooling and (**b**) slow cooling.

Figure 3 shows the particle structures of the hot bands. The size and density of the particles in the hot bands were a function of the contents of Fe and Si in the alloys. In Alloy 1 with 0.09 wt % Fe and 0.035 wt % Si, the particles were rare and small. It could be seen from Figure 3a that only a few particles were scattered on the matrix. With the increase of Fe and Si contents in the alloys, the density of the particles increased correspondingly. In Alloy 2 with 0.25 wt % Fe, the particle volume increased remarkably. Further increasing the contents of Fe and Si gave rise to a significant increase in the amount of particles. In Alloy 3 with 0.5 wt % Fe and 0.25 wt % Si, the dense particles formed a linear structure along the rolling direction (Figure 3c). In Alloy 4 with both high Fe and Si contents, the particles were quite uniform in size and distribution. The volume fraction of the particles was larger than that in Alloy 3. The volume fractions of the particles in the alloys were measured by an image analysis system and shown in Figure 4.

The particles were analyzed by SEM. Figure 5 shows their backscattered electronic images. It could be seen that there were two types of particles distinguished by color. They were marked as I and II, respectively, on the figure. The particles were the broken intermetallics. During hot rolling, the intermetallics that precipitated during casting broke into fragments. In Alloys 1 and 2, the particle structures mainly consisted of type I particles. The type II particles were minor phases and could only be found occasionally. However, in Alloys 3 and 4, both the type I and type II particles were major phases. They bestrewed on the metallographic surfaces. Under high magnification, it could be
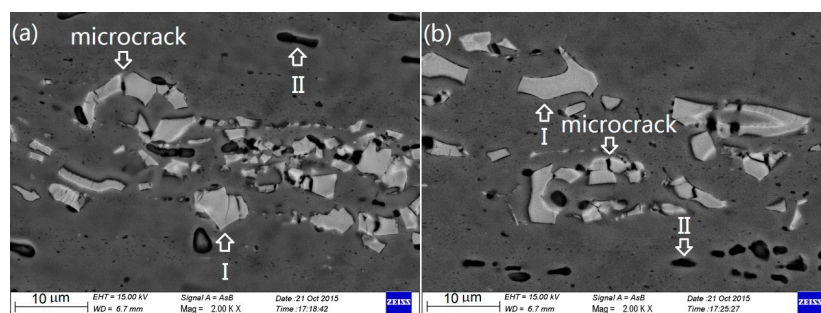
seen that there were many microcracks or cavities between the fragments of the type I intermetallics, especially in Alloy 3.
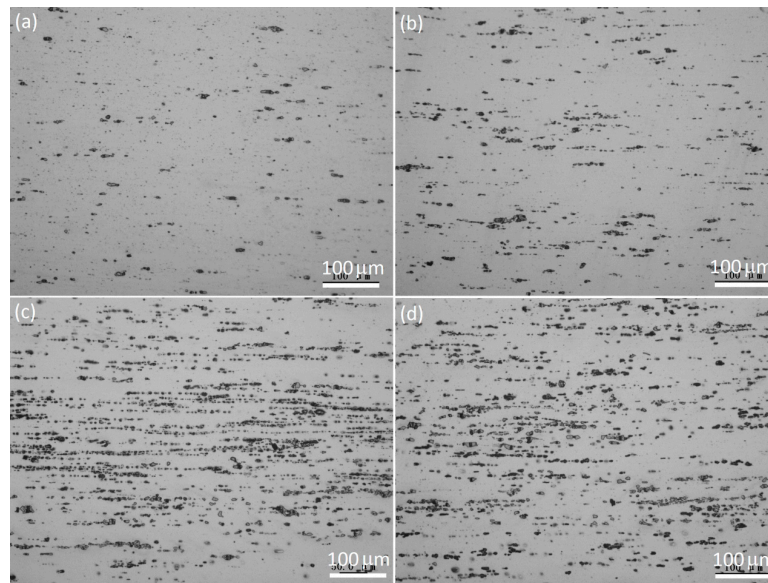
Figure 3. The particles structures of the hot bands. (**a**) Alloy 1; (**b**) Alloy 2; (**c**) Alloy 3; (**d**) Alloy 4.
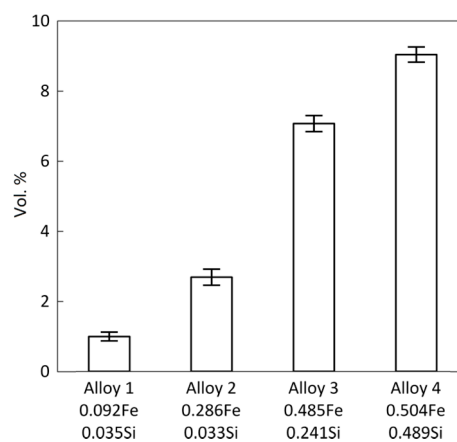
Figure 4. The volume fraction of particles in the alloys.

Figure 5. The backscattered electronic images of the intermetallic particles in (**a**) Alloy 3 and (**b**) Alloy 4.

The compositions of the particles were analyzed by EDX. The results indicated that the type I particles were Al-Mn-Fe particles with a formula close to $Al_6(Fe,Mn)$ in Alloys 1 to 3. Table 2 provides

the typical EDX measurements of the particles. It could be seen that the concentrations of Fe and Mn in the particles varied and the variation was correlated to the Fe content in the alloy. In the low Fe alloy (Alloy 1), the concentration of Fe was quite low. In the medium and high Fe alloys, the concentration of Fe increased remarkably and the composition formula was closer to $Al_6(Fe,Mn)$. In Alloy 4 with high content of Si, the type I particles contained Al, Fe, Mn and Si with a formula close to $Al_6(Fe,Mn)_8Si$.

In the type II particles, Al, Mg and Si were detected by EDX (also see Table 2). However, the composition formula did not fit any of the known phases. According to previous research [2], the type II particles were most likely Mg_2Si phase. The Al detected by EDX was most likely from the Al matrix since the type II particles were fairly small.

**Table 2.** The energy dispersive X-ray (EDX) analysis results of the particles in various alloys, at %.

| Alloy	Type I Intermetallic					Type II Intermetallic		
	Al	Mn	Fe	Si	Mg	Al	Si	Mg
Alloy 1	82.86	11.87	4.51	0.03	1.06	-	-	-
Alloy 2	85.85	8.4	4.62	0.02	1.15	-	-	-
Alloy 3	86.27	7.23	5.5	0.04	0.97	6.51	58.81	32.36
Alloy 4	79.55	6.97	9.37	3.21	0.9	6.96	57.21	33.35

The grain structures of the hot bands and the cold rolled sheets were examined. It was found that all the hot bands were fully recrystallized, as shown in Figure 6, and the grain sizes were related to the contents of Fe and Si in the alloys. With the increase of Fe and Si, the grain sizes decreased, as shown in Figure 7. The grain size of Alloy 4 was much smaller than that of Alloy 1. No recrystallization occurred in the cold rolled sheet during stabilization treatment. They still showed heavy deformed grain structures after being heated at 150 °C for 2 h (Figure 8).
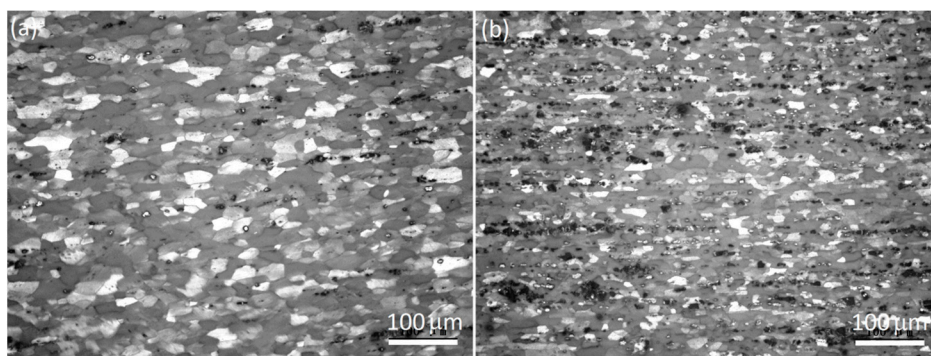
**Figure 6.** The recrystallized grain structures of the hot bands of (**a**) Alloy 1 and (**b**) Alloy 4.
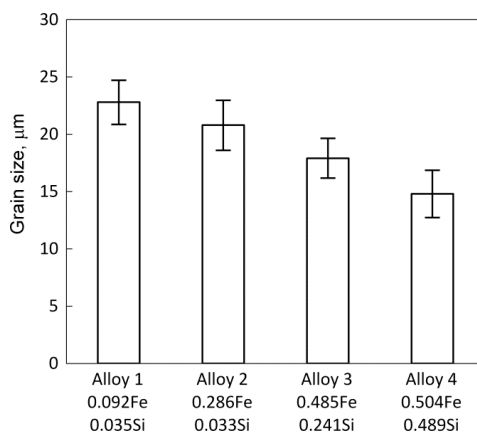
Figure 7. The average grain size of the alloys.
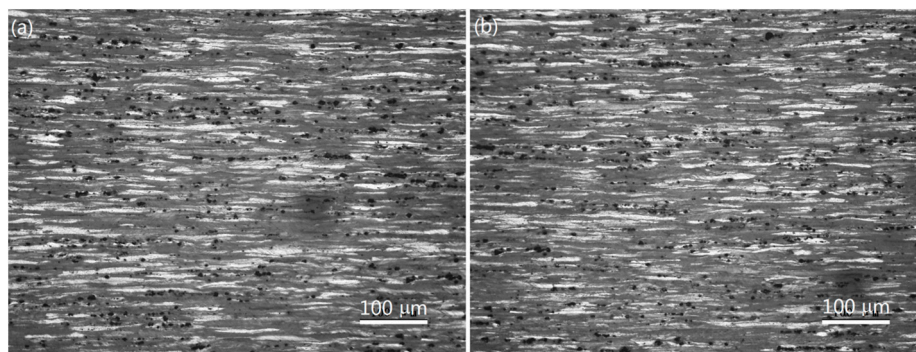
Figure 8. The deformed grain structures of the cold rolled sheets of (**a**) Alloy 3 and (**b**) Alloy 4.

Mechanical Properties

Figure 9a shows the tensile properties of the fully recrystallized hot bands with different Fe and Si contents. It could be seen from the figure that Alloy 1 with low Fe and Si contents demonstrated a best combination of high tensile strength and elongation. Increasing the contents of Fe and Si caused a decrease in the tensile properties. However, the deteriorating extent of the mechanical properties caused by Fe and Si was quite small. Comparing Alloy 1 (with low Fe and Si) to Alloy 4 (with high Fe and Si), ultimate tensile strength (UTS) reduced by 5.2% and elongation (El) reduced by 11.5%. However, on the other hand, the high Fe and Si containing alloy still showed a relatively high tensile strength and elongation: it met the typical mechanical properties of AA5083 alloy at O temper [30]. Figure 9b shows the tensile properties of the cold rolled sheets which were stabilization treated at 150 °C for 2 h. The sheets were subject to heavy deformation and no recrystallization took place during stabilization treatment. Similar to the hot bands, the mechanical properties deteriorated with the increase of Fe and Si. The decrements of the tensile strengths (both ultimate tensile strength and yield strength) were also small, but elongation decreased quite remarkably. The cold rolled sheets were subjected to treatment equivalent to H34. Compared to the typical mechanical properties of AA5083 alloy at H34 temper, Alloy 4 had higher tensile strength and equivalent elongation. This meant that under the condition of casting under near-rapid cooling, the alloy with high Fe and Si contents could still match the typical mechanical properties of AA5083 alloy.
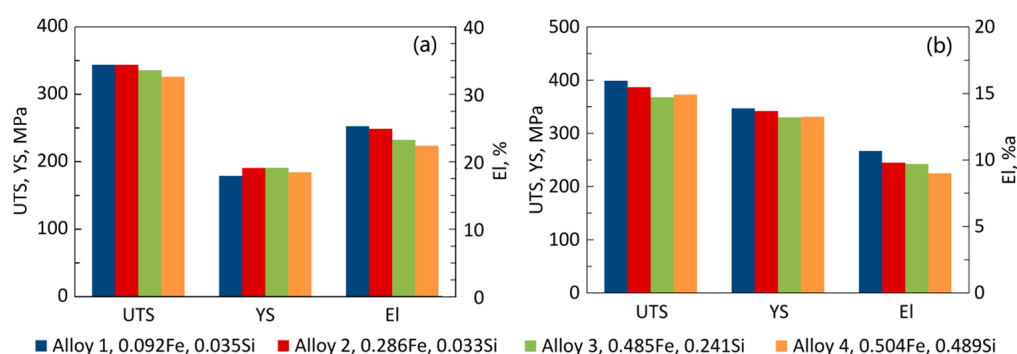

Figure 9. The tensile properties of (**a**) the fully recrystallized hot bands and (**b**) the cold rolled sheets after stabilization treatment.

Figure 10 shows the fracture surfaces of the hot bands revealed by SEM observation. It was found that the fracture features of all the samples exhibited ductile fracture mode at the microscopic level. The fracture surface bestrewed holes and fine dimples. Some particles appeared in the holes. They were the remaining intermetallic particles which were fractured or left from the matrix caused by the material fracturing. With the increase of the contents of Fe and Si in the alloys, the number and size

of holes increased on the fracture surfaces. In the low Fe and Si containing alloy, the holes and the remaining particles were rare and small. In the high Fe and Si containing alloy, it was observed that a large quantity of coarse particles had broken or departed from the matrix. Some secondary cracks were seen on the intermetallic particles in the holes. Figure 11 shows the remaining particles located in the holes and the secondary cracks. These cracks were either from the cavities created during hot rolling, as shown in Figure 4, or created during the fracturing of the materials. However, the secondary cracks did not expand into the matrix. These finding all agreed with the fact that in the high Fe and Si containing alloys, more and coarser intermetallic particles precipitated. Figure 12 shows the fracture surfaces of the cold rolled sheets which were stabilization treated at 150 °C for 2 h. It could be seen that the samples also showed ductile fracture mode at the microscopic level. Similar to the fracture surface of the hot bands, the fracture surface consisted of holes and fine dimples. The holes were filled with intermetallic particles.
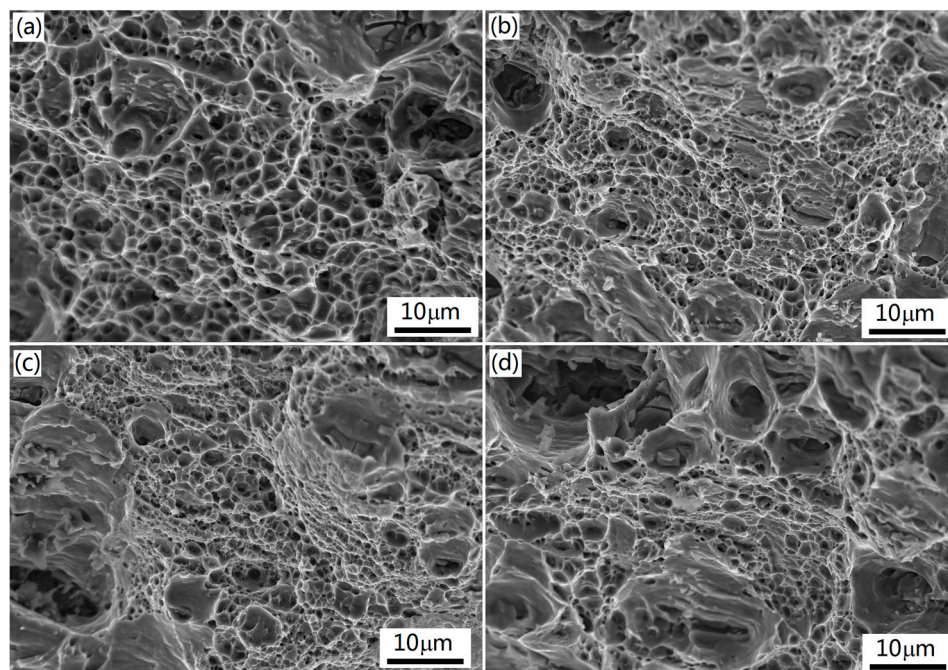
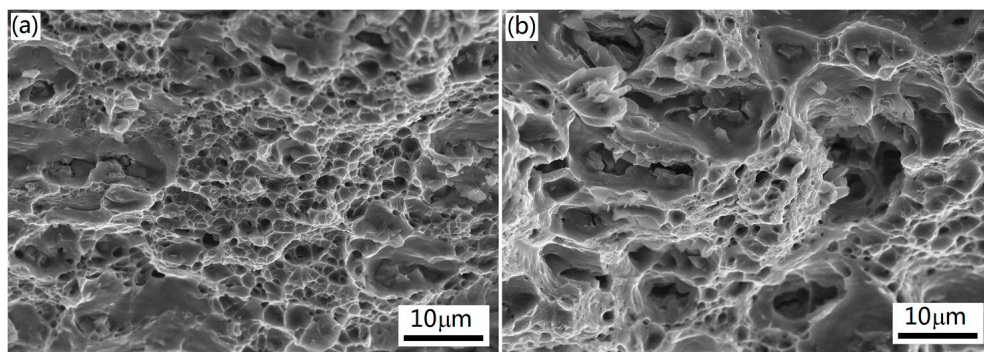
Figure 10. The fracture surfaces of the hot bands. (**a**) Alloy 1; (**b**) Alloy 2; (**c**) Alloy 3; (**d**) Alloy 4.
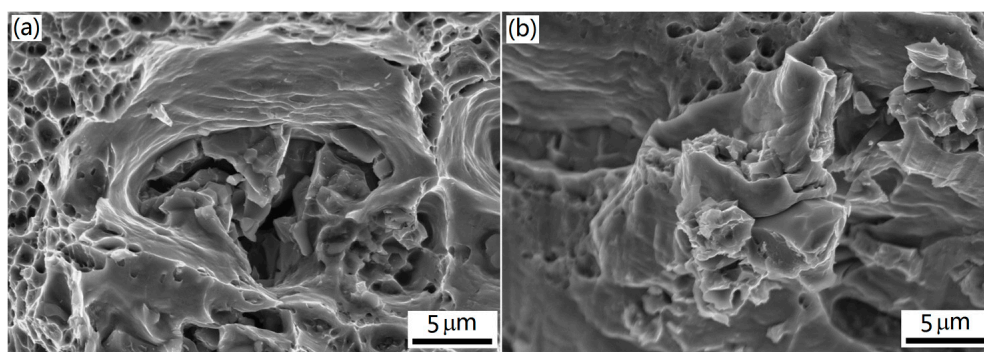
Figure 11. The fractured particles remained in the holes of the fracture surfaces. (**a**) Alloy 3; (**b**) Alloy 4.

Figure 12. The fracture surfaces of the cold rolled sheets stabilizing treated. (**a**) Alloy 2; (**b**) Alloy 4.

4. Discussion

4.1. The Particle Structures

The particle structures in the hot bands were created during hot rolling in which the intermetallics that precipitated during casting were broken into fragments. Therefore, the intermetallic structures of the cast slabs determined the particle structures of the hot bands. In Al-5Mg-0.8Mn alloy, Fe combined with Mn to form intermetallic Al_6(Fe,Mn); Si united with Mg to form intermetallic Mg_2Si. Previous research [2] indicated that the Fe and Si contents and cooling rate were of great effect on the precipitation of intermetallics. In the low Fe and Si alloys, the solidification structures were very simple. The intermetallics that precipitated during solidification were limited. Increasing the contents of Fe and Si gave rise to the significant increase of intermetallics in both amount and size. In the case of slow cooling, the intermetallic Al_6(Fe,Mn) displayed coarse platelet-like structure; Mg_2Si formed integrated networks [2]. The higher the contents of Fe and Si in the alloy, the larger the size and amount of the intermetallics. For example, the fraction of Al_6(Fe,Mn) increased from 0.4% in low Fe alloy to 4.5% in high Fe alloy (0.5 wt % Fe) [2]. The intermetallic Mg_2Si was a minor phase in low Si alloys. In the high Si alloy (0.5 wt % Si), Mg_2Si became the major phase. The intermetallic phases Al_6(Fe,Mn) and Mg2Si were insoluble and could not be removed through heat treatment. Due to their brittle characteristics, the coarse intermetallic phases would fracture into fragments with large size during hot rolling and create microcracks or cavities among the fragments [31]. Therefore, these Fe- and Mn-rich intermetallics had been regarded as most detrimental to the mechanical properties of the alloys [3–5]. In order to minimize the deteriorating influence of the coarse intermetallics on the alloys, the contents of Fe and Si in aluminum alloys were usually limited to a very low level to prevent the precipitation of the coarse intermetallics. For example, the limitations of Fe and Si were 0.4 wt % in the chemical composition specification of AA5083 alloy [1]. In production practices, the actual internal limitations of Fe and Si were usually 0.20 wt %.

On the other hand, in the case of near-rapid cooling, the intermetallics Al_6(Fe,Mn) and Mg_2Si were refined to a significant extent [2]. Even in the alloy with high Fe and Si contents, such as in Alloy 4, the intermetallics precipitated during casting were still very small. The refined intermetallics would break into small fragments and leave fewer microcracks or cavities among the fragments. Therefore, under the condition of near-rapid cooling, in the alloy with higher contents of Fe and Si, the particles were small. In this study, the intermetallics Al_6(Fe,Mn) displayed blocky or flower-like structures in Alloys 1 to 3. They became fish bone or Chinese script morphology in the Alloy 4 with high Fe and Si contents. It was assumed that during hot and cold deformation, these significantly refined intermetallics would break into small fragments and leave limited cavities among the fragments. Especially, in Alloy 4, the fish bone or Chinese script structures of the intermetallic Al_6(Fe,Mn) created uniform sized particles with fewer cavities. It was assumed that these particle structures would be of less deteriorative effect to the mechanical properties of the materials.

4.2. The Mechanical Properties

Alloy 4 with high Fe and Si contents still demonstrated high strength and ductility. The mechanical properties of the alloys cast under near-rapid cooling were not significantly deteriorated by the Fe- and Mn-rich intermetallics. It seemed that the results were not in agreement with the general understanding that increasing the Fe and Mn contents significantly deteriorates the mechanical properties. It was well known that in AA5083 alloy (Al-5Mg-0.8Mn), Fe and Si were impurities; the Fe- and Mn-rich intermetallics were detrimental to the mechanical properties of the alloys. The contents of Fe and Si in the alloy were usually limited to a low level. In this study, the deteriorating effect of the Fe- and Mn-rich intermetallics was reduced. The near-rapid cooling played a key role in this improvement of mechanical properties.

The deteriorating effect of the Fe- and Mn-rich intermetallic on the mechanical properties of the alloys was a function of the size, amount, distribution and morphology of the intermetallic particles that remained and the cavities that formed during deformation. The coarse and sharp particles that remained and the cavities between the fragments worked as the nucleation sites of cracks and gave rise to the premature failure of the materials. In addition, the coarser and sharper the particles and/or the more and larger the cavities among the particles, the severer the deteriorating effect the particles had on the mechanical properties. These characteristics of the particles were determined by the intermetallic phases formed during solidification. Refining the intermetallics and alternating their mass blocky morphologies would reduce the size of the remained particles and minimize the formation of the cavities among the particles. As a result, the detrimental effect of the intermetallic phases on the tensile properties of the alloys could be reduced. In this study, the alloys were solidified at a cooling rate of 20 $^\circ$C·s^{-1} (near-rapid cooling). The intermetallics in the cast slabs were significantly refined, hence, intermetallic particles remained in the rolled products were fine. In this study, although the tensile strengths and elongation of the alloys lowered with the increase of the contents of Fe and Si in the alloys, the decrement was quite small. Therefore, even as the contents of Fe and Si increased to 0.5 wt % (Alloys 3 and 4), the alloys still demonstrated high mechanical properties.

Alloy 4 contained more intermetallic particles than Alloy 3; the cavities among the particles were fewer due to the fish bone structures of the intermetallics formed during near-rapid solidification. The deterioration on the mechanical properties increased from the increased particle number, but decreased from the fewer cavities among the particles. Therefore, the mechanical properties of Alloy 4 decreased further compared to Alloy 3, but to a smaller extent. They still met the typical mechanical properties of AA5083 alloy.

Refining the intermetallics in the high Fe and Si alloys was a good way to minimize the deteriorating effect of the Fe- and Mn-rich intermetallics. This result would be of great interest to the manufacture of AA5083 alloy. Under the condition of near-rapid cooling, a higher level of Fe and Si could be acceptable since the intermetallics formed during casting could be refined by the fast cooling. Therefore, the tolerance of Fe and Si in the chemical composition specification could be widened. Then, more recycled materials with high contents of Fe and Si could be used, which would save production cost.

From a manufacturing viewpoint, in the production of Al-Mg based alloys via continuous strip casting technology, with the advantage of near-rapid cooling, the content limits of Fe and Si could be widened.

5. Conclusions

(1) In the alloys cast under near-rapid cooling, the density and size of the intermetallic particles remained in the hot bands and the cold rolled sheets increases as the contents of Fe and Si increased. However, the increment of the particles sizes is limited due to the refinement of the intermetallics by the near-rapid cooling during casting.

(2)　　The tensile properties of the alloys decreases as the contents of Fe and Si in the alloys increased. However, the decrement of the tensile strengths and ductility is quite small. The strength and ductility of the high Fe and Si containing alloy still met the typical mechanical properties of AA5083.

(3)　　Higher Fe and Si contents could be acceptable in the Al-5Mg-0.8Mn alloy (AA5083 alloy) when the material is cast under near-rapid cooling, such as in the continuous strip casting process, due to its refining effect on the intermetallics.

Author Contributions: All the co-authors of the paper have contributed to the research. Yimeng Sun performed the experiments; Li Zhang operated SEM; Yuhua Zhao, Jijie Wang and Chunzhong Liu contributed the discussion of the experiments; Yulin Liu. designed the experiments and wrote the paper.

Conflicts of Interest: The authors declare no conflict of interest.

References

1.　　The Aluminum Association Inc. *International Alloy Designations and Chemical Composition Limits for Wrought Aluminum and Wrought Aluminum Alloys; AA-TEAL-1-2006*; The Aluminum Association Inc.: Arlington, VA, USA, 2006.

2.　　Liu, Y.; Luo, L.; Han, C.; Ou, L.; Wang, J.; Liu, C. Effect of Fe, Si and cooling rate on the formation of Fe- and Mn-rich intermetallics in Al-5Mg-0.8Mn alloy. *J. Mater. Sci. Technol.* **2016**, *32*, 305–312. [CrossRef]

3.　　Seifeddine, S.; Johansson, S.; Svensson, I.L. The influence of cooling rate and manganese content on the β-Al5FeSi phase formation and mechanical properties of Al-Si-based alloys. *Mater. Sci. Eng. A* **2008**, *490*, 385–390. [CrossRef]

4.　　Sreeja Kumari, S.S.; Pillai, R.M.; Rajan, T.P.D.; Pai, B.C. Effects of individual and combined additions of Be, Mn, Ca and Sr on the solidification behaviour, structure and mechanical properties of Al-7Si-0.3Mg-0.8Fe alloy. *Mater. Sci. Eng. A* **2007**, *460–461*, 561–573. [CrossRef]

5.　　Liu, K.; Cao, X.; Chen, X.G. Tensile properties of Al-Cu 206 Cast Alloys with various iron contents. *Metall. Mater. Trans. A* **2014**, *45*, 2498–2507. [CrossRef]

6.　　Davis, J.R. *Alloying: Understanding the Basics*; ASM International: Materials Park, OH, USA, 2001; p. 382.

7.　　Lennart, B.; Ella, K. *Tamminen Jarmo: Skan Aluminium*; Universitetsforlaget AS: Oslo, Norway, 1986; p. 119.

8.　　Goswami, R.; Spanos, G.; Pao, P.S.; Holtz, R.L. Microstructural evolution and stress corrosion cracking behavior of Al-5083. *Metall. Mater. Trans. A* **2011**, *42*, 348–355. [CrossRef]

9.　　Ramasis, G.; Holtz, R.L. Transmission electron microscopic investigations of grain boundary beta phase precipitation in Al 5083 aged at 373 K 100 °C. *Metall. Mater. Trans. A* **2013**, *44*, 1279–1289.

10.　Harrell, T.J.; Topping, T.D.; Wen, H.; Hu, T.; Schoenung, J.M.; Lavernia, E.J. Microstructure and strengthening mechanisms in an ultrafine grained Al-Mg-Sc alloy produced by powder metallurgy. *Metall. Mater. Trans. A* **2014**, *45*, 6329–6343. [CrossRef]

11.　Lin, Y.; Liu, W.; Wang, L.; Lavernia, E.J. Ultra-fine grained structure in Al-Mg induced by discontinuous dynamic recrystallization under moderate straining. *Mater. Sci. Eng. A* **2013**, *573*, 197–204. [CrossRef]

12.　Verma, R.; Kim, S. Superplastic behavior of copper-modified 5083 aluminum alloy. *J. Mater. Eng. Perform.* **2007**, *16*, 185–191. [CrossRef]

13.　Smolej, A.; Skaza, B.; Dragojevic, V. Superplastic behavior of Al-4.5Mg-0.46Mn-0.44Sc alloy sheet produced by a conventional rolling process. *J. Mater. Eng. Perform.* **2010**, *19*, 221–230. [CrossRef]

14.　Verma, R.; Friedman, P.A.; Ghosh, A.K.; Kim, S.; Kim, C. Characterization of superplastic deformation behavior of a fine grain 5083 Al alloy sheet. *Metall. Mater. Trans. A* **1996**, *27*, 1889–1898. [CrossRef]

15.　Shin, D.H.; Hwang, D.-Y.G.; Oh, Y.J.; Park, K.T. High-strain-rate superplastic behavior of equal-channel angular-pressed 5083 Al-0.2 wt pct Sc. *Metall. Mater. Trans. A* **2004**, *35*, 825–837. [CrossRef]

16.　Singh, D.; Rao, P.N.; Jayaganthan, R. Effect of deformation temperature on mechanical properties of ultrafine grained Al–Mg alloys processed by rolling. *Mater. Des.* **2013**, *50*, 646–655. [CrossRef]

17.　Abdu, M.T.; Dheda, S.S.; Lavernia, E.J.; Topping, T.D.; Mohamed, F.A. Creep and microstructure in ultrafine-grained 5083 Al. *J. Mater. Sci.* **2013**, *48*, 3294–3303. [CrossRef]

18. Topping, T.D.; Ahn, B.; Li, Y.; Nutt, S.R.; Lavernia, E.J. Influence of process parameters on the mechanical behavior of an ultrafine-grained Al alloy. *Metall. Mater. Trans. A* **2012**, *43A*, 505–519. [CrossRef]

19. Roy, I.; Chauhan, M.; Mohamed, F.A.; Lavernia, E.J. Thermal stability in bulk cryomilled ultrafine-grained 5083 Al alloy. *Metall. Mater. Trans. A* **2006**, *37*, 721–730. [CrossRef]

20. Witkin, D.; Han, B.Q.; Lavernia, E.J. Mechanical behavior of ultrafine-grained cryomilled Al 5083 at elevated temperature. *J. Mater. Eng. Perform.* **2005**, *14*, 519–527. [CrossRef]

21. Lin, S.; Nie, Z.; Huang, H.; Li, B. Annealing behavior of a modified 5083 aluminum alloy. *Mater. Des.* **2010**, *31*, 1607–1612. [CrossRef]

22. Yang, D.; Li, X.; He, D.; Huang, H. Effect of minor Er and Zr on microstructure and mechanical properties of Al-Mg-Mn Alloy 5083 welded joints. *Mater. Sci. Eng. A* **2013**, *561*, 226–231.

23. Malopheyev, S.; Kaibyshev, R. Strengthening mechanisms in a Zr-modified 5083 alloy deformed to high strains. *Mater. Sci. Eng. A* **2015**, *620*, 246–252. [CrossRef]

24. Meng, C.; Zhang, D.; Hua, C.; Zhuang, L.; Zhang, J. Mechanical properties, intergranular corrosion behavior and microstructure of Zn modified Al–Mg alloys. *J. Alloys Compd.* **2014**, *617*, 925–932. [CrossRef]

25. Xia, S.L.; Ma, M.; Zhang, J.X.; Wang, W.X.; Liu, W.C. Effect of heating rate on the microstructure, texture and tensile properties of continuous cast AA 5083 aluminum alloy. *Mater. Sci. Eng. A* **2014**, *609*, 168–176. [CrossRef]

26. Liu, W.C.; Morris, J.G. Quantitative analysis of texture evolution in cold-rolled, continuous-cast AA 5xxx-Series aluminum alloys. *Mater. Sci. Eng. A* **2004**, *35*, 265–277. [CrossRef]

27. Zhao, Y.M.; Morris, J.G. Comparison of the texture evolution of direct chill and continuous cast AA5052 hot bands during isothermal annealing. *Mater. Sci. Eng. A* **2005**, *36*, 2505–2515. [CrossRef]

28. García-Bernal, M.A.; Mishra, R.S.; Verma, R.; Hernández-Silva, D. Hot deformation behavior of friction-stir processed strip-cast 5083 aluminum alloys with different Mn contents. *Mater. Sci. Eng. A* **2012**, *534*, 186–192. [CrossRef]

29. Girard, S.X.; Azari, H.N.; Wilkinson, D.S. Effect of thermomechanical processing on grain structure development in a twin-belt strip cast automotive aluminum alloy. *Mater. Sci. Eng. A* **2004**, *35*, 949–952. [CrossRef]

30. Bauccio, M.L. *ASM Metals Reference Book*, 3rd ed.; ASM International: Materials Park, OH, USA, 1999; p. 415.

31. Liu, Y.L.; Kang, S.B. Influence of manganese on microstructure and solidification behavior of aluminum-magnesium alloys. *Mater. Sci. Technol.* **1996**, *12*, 12–18. [CrossRef]